# BEARING CAPACITY CHARACTERISTICS OF GEOCELL REINFORCED SOIL USING DIGITAL IMAGE CORRELATION

Matthew CHUA[1], Takashi KIYOTA[2] and Toshihiko KATAGIRI[3]

**ABSTRACT**: Construction of structures on soft soil presents many challenges for engineers both as designers and contractors. Soil reinforcement has been gaining much attention due to its numerous advantages such as increasing the bearing capacity of soil. Under soil reinforcement, geocells are increasingly used as an alternative to traditional methods. Geocells are defined as a series of interconnected cells typically made up of high-density polyethylene (HDPE). Although there are a number of advantages derived from the use of geocells. The understanding of reinforcing mechanism is still limited. The study investigates the effect of dimensional parameters such as cell opening and cell width on the bearing capacity of square shaped geocell reinforcement based on laboratory model tests along with two-dimensional digital image correlation (2D-DIC).

**Key Words**: *Geocell, Bearing Capacity,* two-dimensional digital image correlation (2D-DIC), Hammock Effect

## INTRODUCTION

Due to the ever-increasing number of construction projects, soil at specific sites may not always be suitable for the needs of the project. Construction of structures on soft soil presents many challenges for engineers both as designers and contractors. Many case studies have been published describing differential settlement and instability problems caused by such soils on a variety of structures ranging from cultural, commercial and residential (Croci, 2000; Kim et al., 2011; Lin et al., 2017; Salcedo & Orozco, 2013).

In such cases, soil improvement needs be conducted to increase bearing capacity and decrease the settlement. Three factors driving the need for soil improvement are the existence of unsuitable soil, lack of space and economic constraints (Gaafer et al., 2015).

Soil reinforcement has been gaining much attention due to its numerous advantages. Under soil reinforcement, geosynthetics are increasingly used as an alternative to traditional methods (Emersleben, 2013; Rowe & Li, 2005). The international geosynthetics society defined different categories of geosynthetics depending on use and method manufacture. Geotextiles, geonets, geomembranes, geocomposites, geosynthetic clay liners, geopipes, geocells, and geofoam are some of the mentioned types (Bathurst, 2009).

The study focuses on the geocell which is a three-dimensional soil confinement system. As shown in Fig. 1, geocells are defined as a series of interconnected single cells usually in the form of a honeycomb structure. They can be made from different materials such as high density polyethylene (HDPE),

[1] Graduate student, Institute of Industrial Science, The University of Tokyo
[2] Associate Professor, Institute of Industrial Science, The University of Tokyo
[3] Technical Director, Institute of Industrial Science, The University of Tokyo

Polyester (PES), or Polypropylene (PP) (Emersleben & Meyer, 2010).

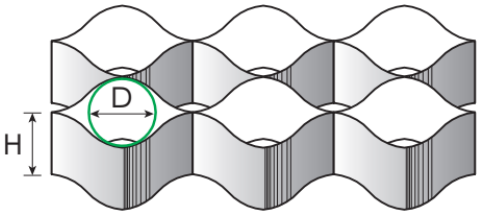


**Figure 1: Geocell system (TokyoInk, 2017)**

Several researchers have presented conceptual theories that explain the advantages of the geocell system over other systems like the geogrid. The structure of the geocell provides all-around confinement to the soil (Emersleben & Meyer, 2010). Stress dispersion occurs as the geocell mattress acts as a platform that redistributes the footing load to a wider geocell area (Zhang et al., 2010). Lastly, the geocell system takes advantage of the so-called hammock effect. This is a result of the vertical displacement in the soil under the geocell mattress, which creates a concave shape in the tensioned material. The curved material has increased stiffness and is anchored laterally. It exerts an upward force that supports the applied loading and improves the bearing capacity (Zhou & Wen, 2008).

The previous studies have conceptually defined some possible failure mechanisms and advantages of geocell. However, there are no realistic observations for these. Thus, the aim of the study is to observe the said mechanisms and understand how changing different geometric properties of the geocell can affect its stress deformation behavior. For this study, a square shaped geocell was also used to investigate the effects of such parameters in the bearing capacity tests. Transparent plastic material was used in fabricating the geocells to be able to observe the particle movements inside the geocell. The square shaped geocell offers a number of good properties such as easier fabrication compared to radial geocells.

The need to directly measure deformation and displacement of soil particles can be costly. Instrumentation is tedious and may provide only limited information for singular or fixed location (Munoz & Kiyota, 2019). The solution is to explore non-contact models. The method that was utilized for this study called Digital Image Correlation (DIC). DIC is a class of non-contact measurement method that analyzes and extracts full field deformation fields based on acquired images that are stored in digital form (Sutton et al., 2009). As a practical and effective tool for quantitative in-plane deformation measure of a planar object surface, two-dimensional digital image correlation (2D-DIC) is now widely accepted and commonly used in the field of experimental mechanics (Senevirathna, 2019). This method can provide full field displacements to sub-pixel accuracy by comparing the digital images of a test object surface acquired before and after the deformation.

## TESTING APPARATUS, MATERIALS AND PROCEDURE

***Loading Apparatus and Soil Box***

For this experimental program, a modified strain-controlled apparatus developed in the Institute of Industrial Science (IIS) of the University of Tokyo was used. It is composed of three main components. These are the soil box, the loading system and the measuring system.

The soil box used is made of aluminum and an acrylic front face panel to observe the inside. The inner dimensions of the box are 670mm in length, 140mm in width, and 580mm in height. The geocell model was embedded 20mm from the surface of the soil. Pressure sensors are also embedded under it to record the pressure experienced by the ground.

The footing used for the test was made of wood with the dimensions of 135mm (length) × 45mm (width) × 45mm (thickness). The length of the footing was made almost equal to the width of the soil box to

maintain plane strain conditions within the test. The length was just enough to pass the wooden block without interference from the side walls of the soil box but was also enough as to not allow out of plane deformation. The base of the footing was made rough by attaching a sheet of sand paper to it. This provision was necessary to avoid slippage between the soil and the footing. The schematic and actual test set up are shown in Fig. 2.

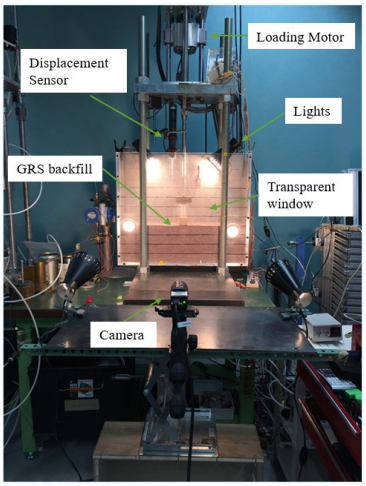


**Figure 2: Experimental Set up**

***Geocell reinforcement model***

Normally, geocell reinforcement is made of dark colored material. This geocell model cannot be used in this study as the particle movement inside the geocell cannot be observed using such a material. The transparent type square-shaped geocell model was used as the reinforcement material. It is characterized by having perpendicular longitudinal and transverse members. Due to the transparent nature of the material, it is advantageous for the purpose of investigating particle movement inside the cell. The material used for this study is made of plastic from clear file folder. This material is commonly used as office supplies and is characterized by its small stiffness. By using this soft material, the effectivity of changing the geometry of the geocell can be thouroughly observed. Fig. 3 shows the schematic of the geocell as well as the orientation of the continues member as indicated by the continuous red arrows.

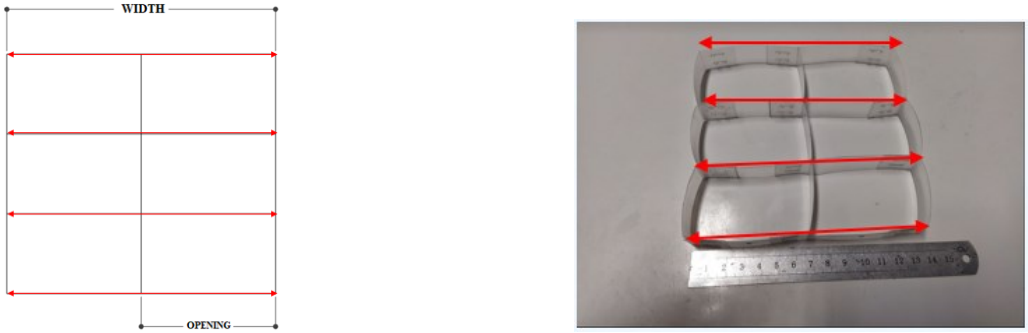


**Figure 3**: **Transparent square-shaped geocell**

***Backfill Material***

The backfill material used for this study is a mix of 50% dyed silica sand no. 5 and normal Silica sand no. 5. The dyed material was used to have the necessary speckle pattern for the digital image correlation. The backfill material can be seen in Fig. 4. Silica sand no. 5 is a kind of natural sand from Seto, Aichi Prefecture (Yu, 2017). Table 1 shows the physical and mechanical properties of Silica sand no. 5. It is classified as poorly-graded sand (SP) according to the Unified Soil Classification System (Yu, 2017). In this study poorly graded soil is used to show that geocell reinforcement can still be used even with poor soil quality.

**Table 1 Properties of Silica Sand no. 5**

| Property | Unit/symbol | Value |
|---|---|---|
| Maximum dry density | g/cm$^3$ | 1.467 |
| Optimum moisture content | % | 17 |
| Minimum Density | g/cm$^3$ | 1.30 |
| Maximum Density | g/cm$^3$ | 1.53 |
| Mean size $D_{50}$ | mm | 0.64 |
| $D_{10}$ | mm | 0.46 |
| $D_{30}$ | mm | 0.54 |
| $D_{60}$ | mm | 0.69 |
| Coefficient of Uniformity, $C_u$ | | 1.5 |
| Coefficient of curvature, $C_c$ | | 0.9 |

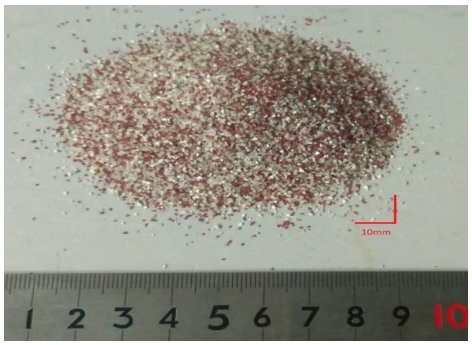


**Figure 4: Dyed silica sand no. 5**

## TESTING PROGRAM

The backfill material was poured into the soil box and compacted in 10mm thick sub layers until the desired total depth of 200mm. Backfilling was temporarily halted to embed pressure sensors and geocell at designated depths. The pressure sensors were placed at depths of 150mm and 100mm levels from the surface of the backfill. The geocell was placed at depth of 60mm from the surface of the backfill. To achieve that target relative density (Dr) of 50% for the backfill material, the target mass of soil was calculated before doing the compaction. The backfill was prepared in thin sub layers to have even compaction. After backfilling up to the 200mm depth, the foundation model described in the previous section was placed at the center of the soil box.

As previously mentioned, to measure the pressure at different depths below the geocell, pressure sensors were embedded in the backfill material. Furthermore, a 10 KN loadcell and Linear Variable. Displacement Transducers (LVDT) were used to record the stress and displacement of the experiment.

Finally, the 2D-DIC setup was done to record and analyze the images from the experiments. The 2D-DIC set up is composed of a stable light source, a highspeed camera, and an adjustable flat stand. The high-speed camera (FUJINON 1:1.4/12.5mm HF12.5SA-1) is fixed on an adjustable flat stand that can be adjusted exactly perpendicular to the acrylic facing. This is then placed over a platform become level with the set up. The lights are also mounted on this adjustable platform to have optimal exposure to the soil box.

Shown in table 2 were the test cases done to examine the effect of geocell opening and width.

**Table 2 Testing Cases**

| Test Symbol | Height (mm) | Opening (mm) | Width (mm) | Orientation of Continue members |
|---|---|---|---|---|
| 1 | 20 | 22.5 | 40 | Parallel to Length of Footing |
| 2 | 20 | 45 | 120 | Parallel to Length of Footing |
| 3 | 20 | 67.5 | 200 | Parallel to Length of Footing |
| 4 | 20 | 22.5 | 40 | Parallel to Length of Footing |
| 5 | 20 | 45 | 120 | Parallel to Length of Footing |
| 6 | 20 | 67.5 | 200 | Parallel to Length of Footing |
| 19 | 20 | 22.5 | 40 | Parallel to Length of Footing |
| 20 | 20 | 45 | 120 | Parallel to Length of Footing |
| 21 | 20 | 67.5 | 200 | Parallel to Length of Footing |
| 35 | 20 | 22.5 | 40 | Perpendicular to Length of Footing |
| 36 | 20 | 45 | 120 | Perpendicular to Length of Footing |
| 37 | 20 | 67.5 | 200 | Perpendicular to Length of Footing |
| 40 | 20 | 67.5 | 202.5 | Perpendicular to Length of Footing |
| 41 | 20 | 67.5 | 270 | Perpendicular to Length of Footing |
| 42 | 20 | 45 | 270 | Perpendicular to Length of Footing |

## RESULTS AND DISCUSSION

### Confinement

To find evidence of confinement, particle movement needed to be followed throughout the test. As shown in Fig. 5, particle movement is clearly halted by the geocell. In the case of planar reinforcements, there is no confinement possible as the soil just moves through and around the reinforcement. Due to this confinement, stiffness is increased which results in the higher capacity.

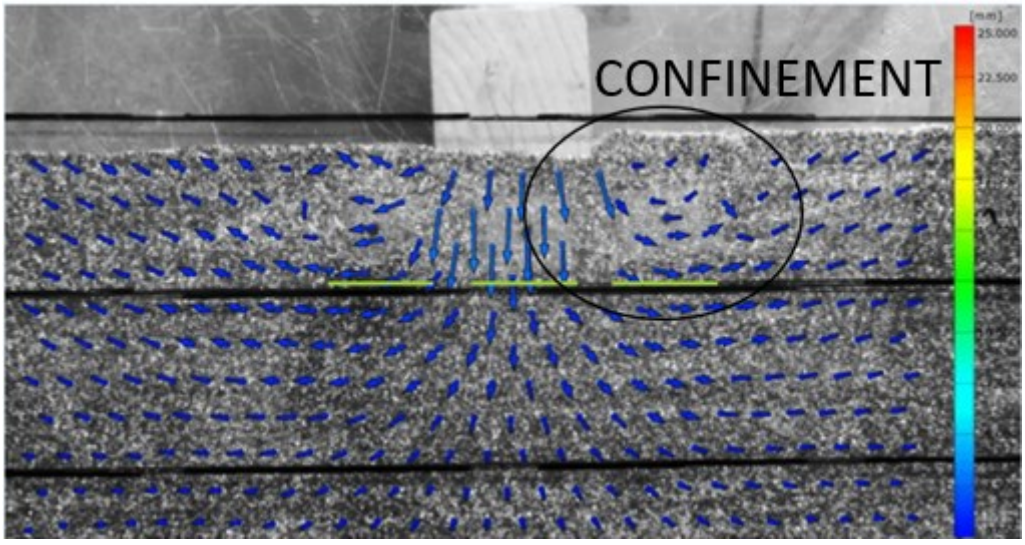


**Figure 5: Image of the geocell confinement effect**

### Stress Dissipation

Stress dispersion is hard to visualize from images. Thus, sensor data is needed to monitor the stress levels under the geocell. Fig. 6 shows the lay out of the pressure sensors. Three sensors are placed just

under the geocell to see how stress varies from the center of the geocell. One sensor was placed under the middle sensor to observe the effect of depth. Based on the pressure readings, stress is significantly decreased under the geocell. Furthermore, stress readings at the middle were found to be higher compared to the sides.

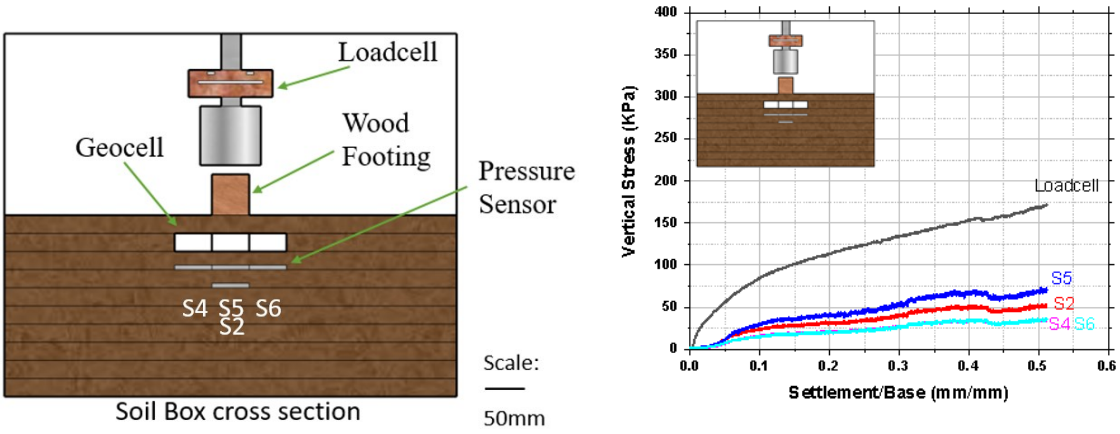


**Figure 6: Sensor data under geocell**

**Hammock Effect**

To investigate the hammock effect, snapshots were taken at different settlement/base stages (S/B=0%, S/B=12.5%, S/B=25%, S/B=50%). The snapshots will show how the deformation progresses and how the hammock effect develops.

Facet points were plotted in at the start of the experiment as a way to track how the particles move throughout the test. Fig. 7 shows the start of the experiment. Fig. 8 shows that at S/B=12.5%, deformation is concentrated at the middle with some slight sideward deformation. The settlement may be due to the loose nature of the backfill. At this stage, some particle movement around the geocell was already observed. The deformation has stopped at around the 50mm mark from the surface. Fig. 9 shows that at S/B=25% S/B mark, a larger deformation area can be observed than that of the 12.5% mark. Settlement can be observed to have stopped at around the 7.5cm mark from the surface. At this stage, visible start of heaving can be seen. Sideward progression of deformation can be seen to progress while vertical deformation halting. This could be the evidence for the hammock effect. Fig. 10 shows at S/B=50% S/B mark, deformation seemed to have reached the 100mm mark below the surface. At this point, there is visible transfer of the deformation from vertical to horizontal. This is where the hammock effect more evident. Although the deformation seems to be excessive, the stress deformation behavior for these cases showed a hardening behavior, thus the hammock effect could be still developing even at this point.

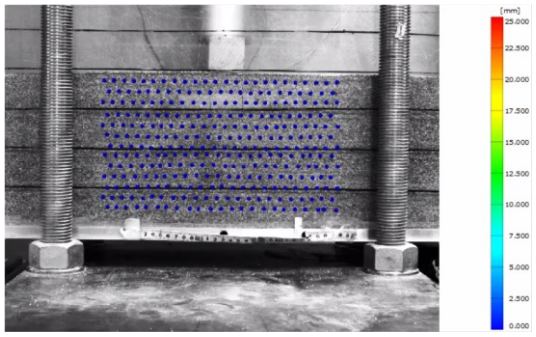

**Figure 7: S/B=0%**

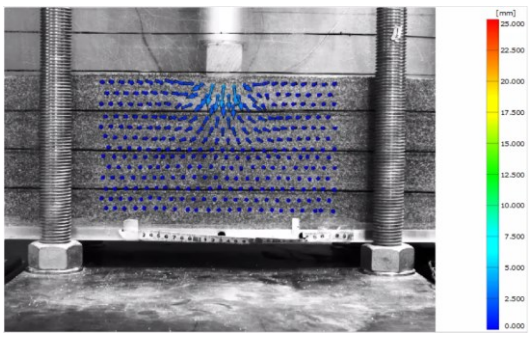

**Figure 8: S/B=12.5%**

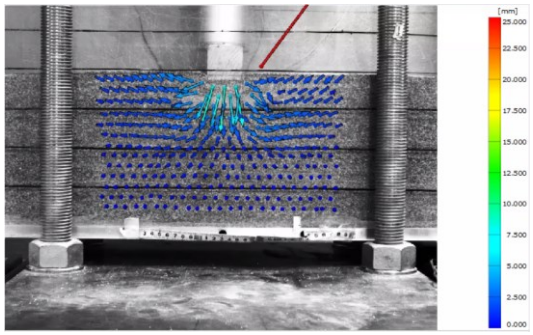

Figure 9: S/B=25%

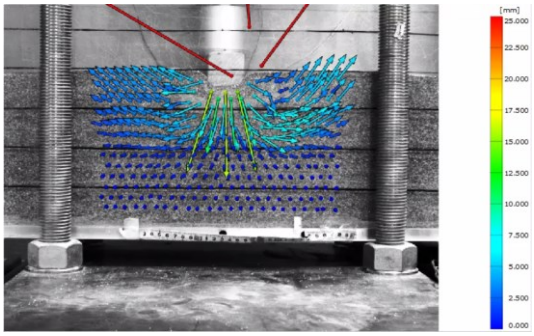

Figure 10: S/B=50%

**Effect of width**

To investigate the effect of the geocell width, samples were prepared using the same opening size while varying the width. As shown in Fig 11, the effect of width is negligible at low strain levels (i.e. 0 to 0.2 S/B). After which a more complex mechanism is activated. By increasing the width, mattress stiffness is decreased. However, a wider geocell would also mean that at larger settlements more anchorage can be activated. Moreover, the hammock effect is also activated at larger settlements. To activate significant hammock effect, wider geocells need larger vertical settlement. Based on these results, increasing the width can only be effective up to certain width and settlements. A geocell width of three times that of the foundation seemed to produce the best results.

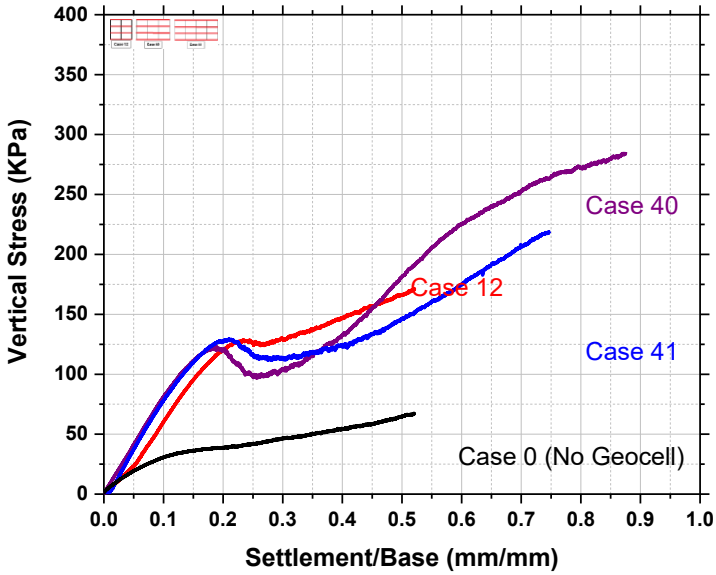


**Fig 11: Relationship between S/B and vertical stress (varying width)**

**Effect of opening**

To check the effect of the geocell opening size, samples were prepared with the same width while varying the opening size. As shown in Fig 12, by decreasing the opening size, strength can be increased. Relatively high stiffness is generally maintained until S/B=0.15. The peak strengths were recorded as 275 kPa, 200 kPa, and 175 kPa for cases 1,2, and 3 respectively.

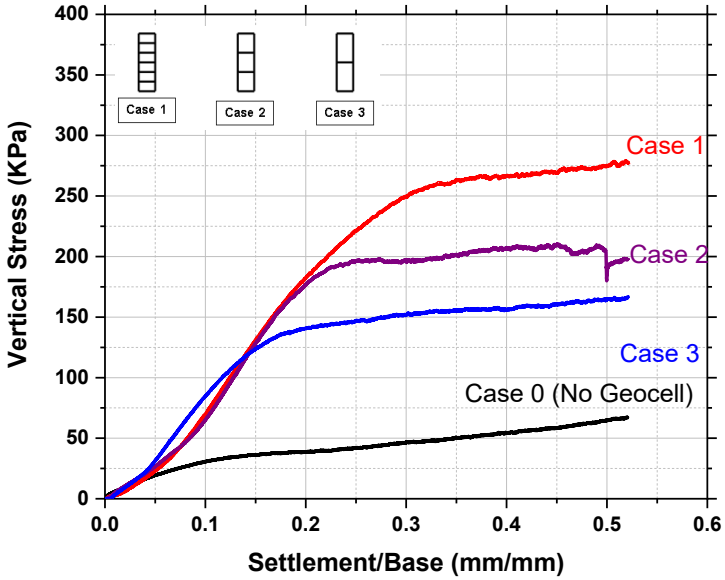


**Figure 12: Relationship between S/B and vertical stress (varying opening)**

## CONCLUSIONS

Considering the bearing capacity characteristics of square-shaped geocell reinforcement, the response of the foundation varied depending on several factors. The relationship between S/B and vertical stress of several tests were compared and analyzed to determine the effect of geocell width and opening.

It was determined from the series of tests that by decreasing the opening size of the geocell pockets, a stiffer and more resilient foundation may be achieved. This finding was consistent with all the results from the experiments. Furthermore, there was no upper or lower limit found for this parameter based on the experiments.

It was determined from the series of tests that by increasing the width of the geocell, some strength gain is achieved up the three times the width of the foundation width. This meant that increasing the geocell width was only effective to a certain point. An interesting finding is that even for a geocell with width equal to that of the foundation width, large improvement in the bearing capacity was still observed.

## REFERENCES

Bathurst, R. . (2009). Geosynthetics Classification. *International Geosynthetics Society*, 1–2.

Croci, G. (2000). General methodology for the structural restoration of historic buildings: The cases of the Tower of Pisa and the Basilica of Assisi. *Journal of Cultural Heritage*, *1*(1), 7–18. https://doi.org/10.1016/S1296-2074(99)00119-3

Emersleben, A., & Meyer, N. (2010). Verification of the load transfer mechanism of geocell reinforced soil in large scale model tests and different in-situ test fields. *Geotechnical Special Publication*, (199), 1670–1679. https://doi.org/10.1061/41095(365)169

Emersleben, Ansgar. (2013). Analysis of Geocell load transfer mechanism using a new radial load test. *Geotechnical Special Publication*, (230), 346–358. https://doi.org/10.1061/9780784412770.023

Gaafer, M., Bassioni, H., & Mostafa, T. (2015). Soil Improvement Techniques. *International Journal of Scientific & Engineering Research*, *6*(12), 217–222. https://doi.org/10.1007/978-3-319-53429-9_5

Kim, Y. J., Gajan, S., & Saafi, M. (2011). Settlement rehabilitation of a 35-year-old building: Case study integrated with analysis and implementation. *Practice Periodical on Structural Design and Construction*, *16*(4), 215–222. https://doi.org/10.1061/(ASCE)SC.1943-5576.0000092

Lin, L., Hanna, A., Sinha, A., & Tirca, L. (2017). High-rise building subjected to excessive settlement of its foundation: A case study. *International Journal of Structural Integrity*, *8*(2), 210–221. https://doi.org/10.1108/IJSI-05-2016-0019

Munoz, H., & Kiyota, T. (2019). Deformation and localisation behaviours of reinforced gravelly backfill using shaking table tests. *Journal of Rock Mechanics and Geotechnical Engineering*. https://doi.org/10.1016/J.JRMGE.2019.06.008

Rowe, R. K., & Li, A. L. (2005). Geosynthetic reinforced embankments on soft foundations. *Geosynthetics International*, *12*(1), 50–85.

Salcedo, M. Q., & Orozco, L. F. R. (2013). Differential Settlement Problem of a Large Apartment Building in Bogotá , Cause and Solution. *International Conference on Case Histories in Geotechnical Engineering*, (2), 1–6.

Senevirathna, N. K. R. (2019). Study on pull-out behaviour of square-shaped geocell reinforcement embedded in backfill using two-dimensional digital image correlation. The University of Tokyo.

Sutton, M., Orteu, J.-J., & Schreier, H. (2009). *Image Correlation for Shape, Motion and Deformation Measurements: Basic Concepts, Theory and Applications*. Boston, MA: Springer-Verlag US.

TokyoInk. (2017). *グランドセル ® Groundcell*.

Yu, F. (2017). Characteristics of particle breakage of sand in triaxial shear. *Powder Technology*, *320*, 656–667. https://doi.org/10.1016/j.powtec.2017.08.001

Zhang, L., Zhao, M., Shi, C., & Zhao, H. (2010). Bearing capacity of geocell reinforcement in embankment engineering. *Geotextiles and Geomembranes*, *28*(5), 475–482. https://doi.org/10.1016/j.geotexmem.2009.12.011

Zhou, H., & Wen, X. (2008). Model studies on geogrid- or geocell-reinforced sand cushion on soft soil. *Geotextiles and Geomembranes*, *26*(3), 231–238. https://doi.org/10.1016/j.geotexmem.2007.10.002